Journal of Environmental Chemical Engineering 8 (2020) 103669

Contents lists available at ScienceDirect

Journal of Environmental Chemical Engineering

journal homepage: www.elsevier.com/locate/jece

Synthesis, characterization and life cycle assessment of carbon nanospheres from waste tires pyrolysis over ferrocene catalyst

Ava Heidari[a,*], Habibollah Younesi[b]

[a] Department of Environmental Science, Faculty of Natural Resources and Environment, Ferdowsi University of Mashhad, Mashhad, Iran
[b] Department of Environmental Science, Faculty of Natural Resources, Tarbiat Modares University, Tehran, Iran

ARTICLE INFO

Keywords:
Life cycle assessment
Carbon nanospheres
Waste tire
Characterization
Recycling

ABSTRACT

Waste tires can be a promising carbon precursor for the production of carbon nanospheres (CNSs) because of their high carbon content, low price, and abundance. CNSs were synthesized from waste tire powder through a chemical vapor deposition method over the ferrocene catalyst at 800 − 900 °C. The scanning electron microscope (SEM), transmission electron microscopy (TEM), X-ray powder diffraction (XRD), Fourier-transform infrared spectroscopy (FTIR), Brunauer-Emmett-Teller (BET), and Raman spectroscopy analyses characterized the as-synthesized CNSs. The obtained products had a spherical shape with a mean size of 50 nm. The least BET surface area, the total pore volume, and relative intensities of D- and G-bands (I_D/I_G) of the CNSs were found to be 65 m^2/g, 0.73 cm^3/g, and 0.98. Decreasing heating temperature and increasing residence time resulted in higher the BET surface area. The environmental burdens of the CNSs manufacturing from waste tire powder were assessed by a cradle-to-gate life cycle assessment (LCA) method, at the early stage of development. The results showed that climate change with 0.141 kg CO_2 eq (for S1 sample) and 0.287 kg CO_2 eq (for S2 sample) was the most detrimental effect of CNSs synthesis. S2 had the largest product environmental footprint (PEF) value of 21.1 compared to the S1 with a quantity of 12.3. The CNSs synthesis phase had the maximum environmental impact in the life cycle of S2. Among all materials, electricity consumption in the process was a significant contribution (more than 70 %) in categories such as eutrophication, climate change, and acidification. According to cumulative energy demand (CED), a total of 3.7 and 5.9 MJ were required to produce 1 g of S1 and S2 samples, respectively in which 3.3 and 5.3 MJ were non-renewable energy. Therefore, to improve the environmental proficiency of the system, the temperature and the time required for the feedstock conversion and CNSs synthesis processes should be declined.

1. Introduction

In recent years, carbon-based nanomaterials with different shapes and structures have been synthesized and characterized for example carbon nanotubes [1], carbon nanofibers [2], mesoporous carbon [3], graphene [1], fullerenes [4], and carbon spheres (CNSs) [5]. Among different shapes, CNSs are attracting interest due to high surface area, high packing density, excellent electrical conductivity, and high thermal stability. Until now, these materials have been used as catalyst supports, column packing, lubricating materials, biomedical drug carriers, fillers for polymer composites, etc. [6–10]. The spherical bodies can be categorized based on their morphology (as solid, core-shell or hollow), texture (indicating concentric, radial or random arrangement of the carbon layers), and size (2–20 nm; carbon onions, 50–1000 nm; carbon nanospheres, and > 1000 nm; carbon beads) [5].

CNSs have been synthesized by different methods, such as Chemical Vapor Deposition (CVD) [11,12], arc discharge [13], shock compression [14], and laser ablation [15]. CVD method is a promising technique due to the ease of scale-up, low-cost, low synthesis temperatures, and control in synthesis parameters [16]. Moreover, an economical way for the mass production of CNSs under reasonable experimental conditions is still required. Hence, the carbon precursor and the engineered techniques are the two crucial subjects for the improvement of the eco-friendly and inexpensive production process of CNSs [17]. Some studies utilized petroleum products such as acetylene [18], methane [19], toluene [16], and polystyrene [20], as a carbon source for CNSs synthesis. The disadvantages of these feedstocks for CNSs production were the generation of a significant amount of unwanted byproducts, new purification stages, low yields, high-energy requirements, high fabrication costs, etc. Therefore, earlier researches have been emphasized on

* Corresponding author.
E-mail address: heidari@um.ac.ir (A. Heidari).

https://doi.org/10.1016/j.jece.2020.103669
Received 30 September 2019; Received in revised form 26 December 2019; Accepted 6 January 2020
Available online 07 January 2020

alternate carbon sources such as sucrose [21], biowaste [12], and polymeric waste [20,22].

In order to find new carbon precursors for preparation for CNSs, waste tire powder can be considered because it contains a high amount of carbon (more than 80 %) [23–25]. Recently, the synthesis of new valuable products such as carbon nanostructures through a pyrolysis process has been reported in the literature [24,26–36]. For example, Yang et al. [37] synthesized carbon nanotubes from waste tire through the CVD method over cobalt catalysts. Also, Zhang et al. [24] and Zhang and Williams [38] successfully produced carbon nanotubes from scrap tire over different catalysts (Co/Al_2O_3, Cu/Al_2O_3, Fe/Al_2O_3, and Ni/Al_2O_3) by pyrolysis-catalysis process. Besides, Maroufi et al. [22] converted waste tire rubber to carbon nanoparticles at 1550 °C. However, production at such a very high carbonization temperature is very costly. These findings have encouraged us to try a new synthetic method that allows preparation CNSs from waste tire powder at a relatively lower temperature.

Manufacturing is crucial to a sustainable world economy. Any new materials or technologies should be developed based on the principles of sustainable development [39]. The nanomaterials and nanotechnology provide new and efficient solutions to global challenges including green manufacturing and chemistry, materials supply and utilization, water purification, clean energy technologies, etc. [40]. Moreover, drawbacks may be created from the massive energy and resource consumption in the manufacturing phase and CO_2 emission associated with life cycles of nanomaterials [41–43]. It is therefore essential to understand the unknown health risk and the environmental impacts of these materials [41,44–46]. Life cycle assessment (LCA) displays a comprehensive framework that calculated the potential environmental impacts of a product over its complete life cycle using a well-defined and documented methodology [47,48]. Recently, some researches have been reported the LCA of Fe_3O_4 nanoparticles [49], MoS_2 nanoparticles [50], carbon nanofiber [51,52], carbon nanotube [53–55], graphene [56,57], and a number of nanoproducts [58–61]. However, there is still restricted quantitative data on the application of the LCA approach to determine issues from other nano components manufacturing such as carbon sphere. The previous studies paid particular attention to the synthesis and characterization of CNSs. There is a lack of data regarding the impact of precursor and process parameters on the environmental and energy burdens of CNSs which was considered by this study.

The current study focuses on the preparation of CNSs by a catalyst pyrolysis procedure from waste tire powder. The as-prepared CNSs were determined using different techniques (SEM, TEM, XRD, Raman, FTIR, BET). Moreover, LCA was utilized to identify and measure a number of environmental burdens related to the synthesis process from cradle-to-gate. To the best of our knowledge, this is the first study that simultaneously investigated the synthesis, characterization and, the environmental impact assessment of CNSs.

2. Martial and method

2.1. Synthesis of CNSs

Waste tire powder was taken from a tire factory (Yazd Tire, Iran). The chemical materials such as Ferrocene, n-hexane, and toluene were purchased from Merck Company (Germany). Experiments were carried out in a horizontal ceramic furnace. The process for waste to CNSs generation involved two stages: (1) Feedstock preparation and (2) Catalytic pyrolysis of feedstock. In the first step, the waste tire powder was carbonized under N_2 gas flow in two ways. The condition of the furnace (e.g., temperature, heating rate, residence time, and gas flow rate) for the synthesis of the CNSs are summarized in Table 1. After carbonization time passed and the reactor was cooled to ambient temperature, the obtained solid was immediately placed on ice to remove its N_2 gas. Next, it was grounded and sieved. In order to obtain a fine particle, the product was dispersed in water and put into the ultrasonic bath. Afterward, a very fine particle was separated from it. This stage was repeated several times. Finally, the resulting material was dried at room temperature.

Table 1
The condition of the furnace for the synthesis of the CNSs from the waste tire powder.

Parameters	S_1		S_2	
	Preparation of feedstock	CNSs synthesis	Preparation of feedstock	CNSs synthesis
Temperature (°C)	500	900	400	800
Heating rate, (°C/min)	30	30	30	30
Residence time (h)	2	0.25	0.16	3
Flow rate of N_2 (L/min)	3	3	3	3

In the second step, first, the carbonized waste tire powder and ferrocene (catalyst) were mixed with two weighting ratios (1:20 and 1:17) in n-hexane. Next, the resulting suspension was stirred at room temperature and then placed in the ultrasonic bath for 15 min to form a homogeneous slurry. After that, the mixture was dried in an oven at 70 °C to remove the remaining solvent before pyrolysis. Subsequently, it was placed inside a ceramic boat and inserted in the center of the reactor in a furnace. Following this, the sample was pyrolyzed under the given conditions (Table 1). Finally, the solid material was collected from the quartz tube and kept in the bottle for characterization. Generally, CNSs samples were synthesized based on two different procedures denoted as S_1 and S_2. To purify and remove the metal nanoparticles from CNSs, the synthesized materials were dissolved in concentrated hydrochloride acid and nitric acid solution for about 16 h at room temperature. The final product dried at 40 °C overnight. The yield of CNSs production was about 33 percent.

The morphology and the size of the carbon products were considered by a Field Emission Scanning Electron Microscope (FE-SEM) (MIRA3, TESCAN, Czech Republic) and Transmission Electron Microscopy (TEM) (CM120, Philips, Holland). The crystal structure of the samples was determined with an X-ray diffractometer (PW1730, Philips, Netherlands) using Cu-Ka radiation at $\lambda = 1.54060$ Å. The functional groups of the CNSs samples were characterized by Fourier-transform infrared (FTIR) spectroscopy (BRAIC, WQF-510, China). The data were taken in the range of $400-4000\ cm^{-1}$ using the KBr. The intramolecular vibration mode of CNSs molecules was examined with Raman spectroscopy (Takram P50C0R10, Teksan, Turkey) at a wavelength of 532 nm between 100–4400 (cm^{-1}). The porosity and pore structures of the CNSs samples were identified by a micromeritics ASAP 2010 instrument (BELSORP-mini II, MicrotracBEL, Japan) using N_2 adsorption-desorption isotherms. The surface area and pore size distribution were calculated by Brunauer–Emmet, and Teller (BET) and Barrett–Joyner–Halenda (BJH), respectively. The samples degassed at 120 °C for 24 h. The mean crystalline size of as-synthesized CNSs was determined by Scherrer's formula as follows [62]:

$$T = \frac{K\lambda}{\beta Cos\Theta} \quad (1)$$

where T is the mean particle size, K is Scherrer's constant, λ is the X-ray wavelength, β is the full width at the half maximum intensity of the peak (FWHM) and Θ is the Bragg angle.

2.2. LCA methodology

The goal of the work is to assess the life cycle environmental burdens of CNS_s production from the waste tire (S1 and S2 samples). The functional unit was the production of 1 g of CNSs. This is similar to that

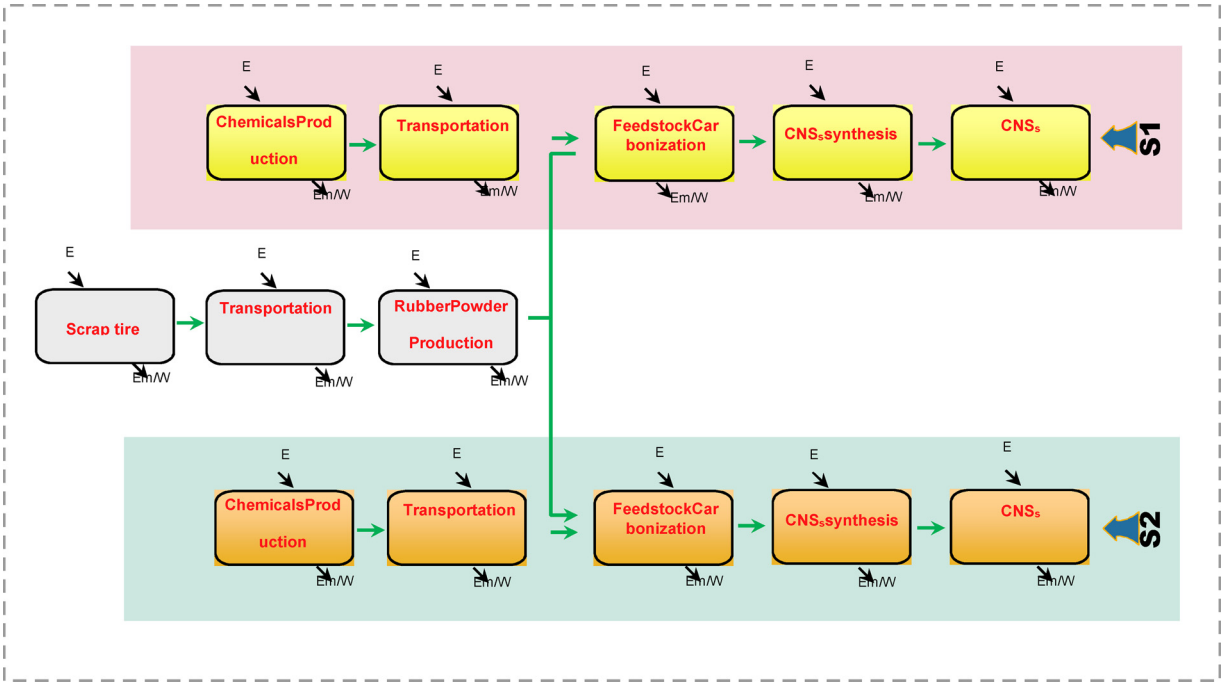

Fig. 1. The system boundary for CNSs production from the waste tire.

utilized in Cossutta et al. [56] study for graphene production. Fig.1 presents the system boundary for CNSs production from the waste tire. It included processes from raw materials extraction, transportation, and processing through to CNSs production. End-of-life activities for CNSs were excluded from the analysis. The scope was "cradle-to-factory gate", which was assumed by following a published procedure [56,63]. Data for the waste tire recycling process were taken from a recycling plant in Mashhad, Iran. The inventory data of materials and energy for CNS_s synthesis, which summarized in Table S1, were obtained from laboratory experiments, as mentioned above. Trucks with a capacity of 16 metric tons that fueled by Euro-4 diesel were considered for transporting of materials. A 250 km road route was assumed to transport materials to the plant. The electricity needed for the processes was assumed to be provided by the national power grid. Inputs for infrastructures are beyond the scope of this work. Virgin materials and energy sources data were gotten from the database of the Ecoinvent 3.4 database.

The three applied assessment methods for analyzing the life cycle impact assessment were the PEF, the CML 2001, and CED. PEF was developed by EC as a more harmonized agenda for labeling green products [64]. The environmental impact categories were climate change (CC), ozone depletion (OD), ionizing radiation (IR), photochemical ozone formation (POF), respiratory inorganics (RI), noncancer human health effects (NCHHE), cancer human health effects (CHHE), acidification terrestrial and freshwater (ATF), eutrophication freshwater (EF), eutrophication marine (EM), eutrophication terrestrial (ET), ecotoxicity freshwater (ETF), land use (LU), water scarcity (WS), resource use, energy carriers (RUEC), and resource use, mineral and metals (RUMM). Besides, the CED represents the direct and indirect energy consumed over the life cycle of a product. CML (Developed by the Institute of Environmental Sciences of Leiden University) 2001 is a problem-oriented method with eleven impact categories in the baseline version (Fig. S3). The LCA model was modeled by Simapro 9.0 software.

3. Results and discussion

3.1. CNS synthesis

3.1.1. SEM and TEM analyses

The morphology of the as-synthesized CNSs from waste tire powder has been analyzed by FE-SEM and TEM analyses. As shown in Fig. 2 (a and b), most of the as-synthesized CNSs have smooth surfaces, no porosity accessible to the surface, relatively narrow size distribution, and nearly spherical shape. The TEM images (Fig. 3) were also confirmed a similar configuration for both CNSs samples. These carbon spheres have an average diameter of 38 and 40 nm for S1 and S2, respectively. The SEM and TEM images of CNSs manufactured at various annealing conditions exhibited that the temperature does not significantly affect the morphology and the size distribution. Similar characteristics have been demonstrated for CNSs in previous studies [18,20,21]. For instance, Supriya et al. [12] reported carbon nanospheres with a diameter of 40 – 60 nm from Lablab purpureus seeds (as carbon source) by the pyrolysis method. Besides, Manaf et al. [17] fabricated CNSs with a diameter of 50–60 from natural biowaste sago hampas. Maroufi et al. [22] synthesized spherical carbon shaped particles with a diameter of 20–50 nm from waste rubber.

3.1.2. XRD analysis

Fig. 4 displays X-ray diffraction patterns of synthesized CNS_s from the waste tire powder. The distinct peaks appearing at 2Θ of 25° (for S1) and 24.8° (for S2) are the reflections from 002 plane which ascribed to graphite carbon with the highly ordered crystalline structures (ICDD 10777164). The interlayer d-spacing (d_{002}) of the sample which applied as a quantitative measurement of the graphitic character, is 3.54 (for S1) and 3.58 (for S2) Å. Other peaks at 41.8° (for S1 and S2) and 43.3° (for S2) with interlayer d spacing of 2.15 and 2.08 Å indicated the (101) and (001) planes. They are related to sp^2 structures of carbon. These results are inconsistent with previous studies [12,65,66] which synthesized the carbon nanosphere from different waste.

3.1.3. Raman analysis

Raman spectra of the as-synthesized CNS_s from waste tire powder were shown in Fig. 5. The Raman spectra of samples display two main

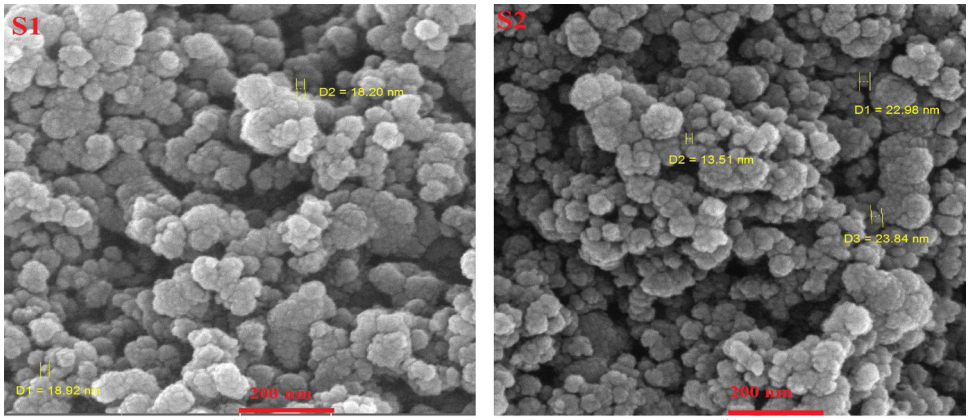

(a) (b)

Fig. 2. SEM images of the as-synthesized CNSs from waste tire powder at 900 °C for 0.25 h (S1; (a)) and 800 °C for 3 h (S2; (b)) in N_2 atmosphere.

similar peaks diagnostic of disorder in the carbon structure symbolized as D- and the diagnostic of structural order symbolized as G- bands. The D-band was detected at 1354 cm^{-1} and 1349 cm^{-1} for S1 and S2 samples, respectively. It is related to the vibration of the carbon atoms with dangling bonds which indicate cumulative disorders in the carbon structure [67]. Also, the G-band at 1576 cm^{-1} and 1581 cm^{-1} can be seen in the spectra of S1 and S2 samples, respectively. This band, however, corresponded to sp^2 hybridized carbon atoms from stretching modes of C═C of the E_{2g} mode of graphite [68,69]. To determine the degree of graphitization, the relative intensities of D- and G- bands (I_D/I_G) were computed from their peak heights. The I_D/I_G was found to be 0.981 and 0.982 for S_1 and S_2 samples, respectively. The I_D/I_G obtained in this study was higher than those reported by Atchudan et al. [21], Chandra Kishore et al. [18], and Hegde et al. [66].

3.1.4. FTIR analysis

Fig. 6 shows the FTIR spectra of the as-synthesized CNSs from waste tire powder. The surface of both CNSs samples exhibited the same functional groups including C−OH, −OH, C═C, and C–H groups. The peaks at 872 cm^{-1} were related to C–H stretching vibrations [70]. The broad strong bands between 1000 and 1400 cm^{-1} correspond to the bending vibrations of C−OH [71,72]. The vibrations at 1580 cm^{-1} were attributed to the C═C group indicating the graphitic nature of the obtained nanoparticles [12,17]. Besides, the bands at around 3550 cm^{-1} were ascribed to stretching vibrations of −OH [73]. In addition, the absorption peak at 510 cm^{-1} was appeared due to the presence of some oxide particles [66].

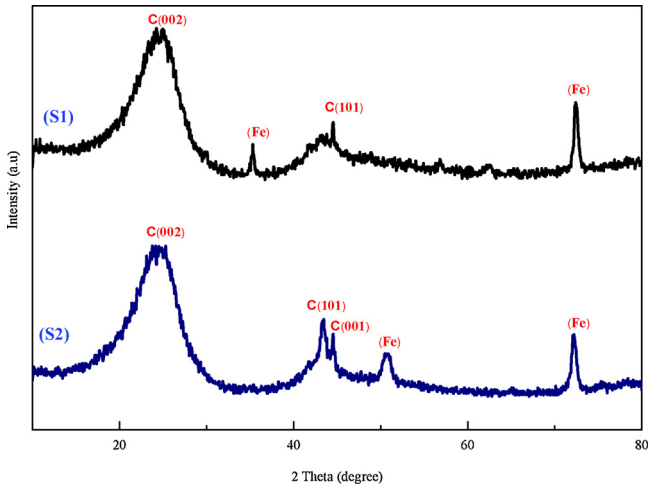

Fig. 4. XRD diffraction patterns of the as-synthesized CNSs from waste tire powder at 900 °C for 0.25 h (S1) and 800 °C for 3 h (S2) in N_2 atmosphere.

3.1.5. BET analysis

Fig S1(a) depicts the N_2 adsorption/desorption isotherms and the corresponding BJH pore size distribution of the as-synthesized CNSs from waste tire powder. According to IUPAC classification, isotherms of two samples follow type III, indicating non-porous materials [74]. The hysteresis loops seen at relatively high pressures have the shape of the type H_3, which manifests the solid samples with a very wide distribution of pore [74,75]. Similar results were obtained for carbon spheres,

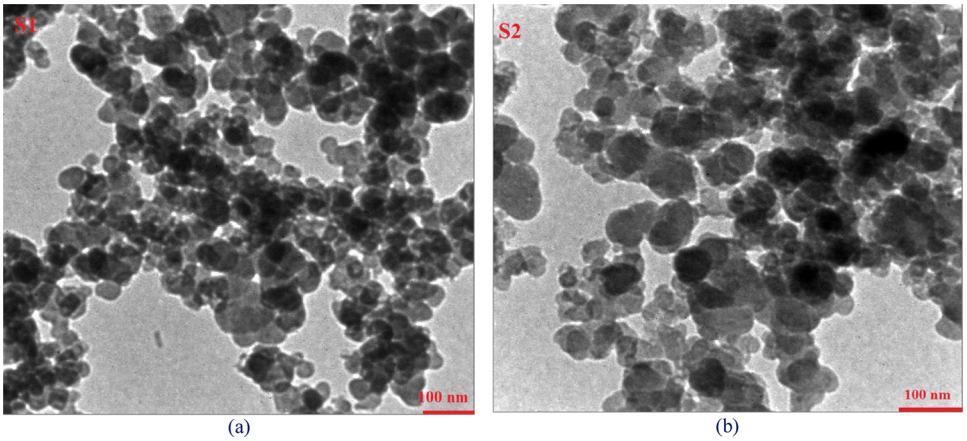

(a) (b)

Fig. 3. TEM images of the as-synthesized CNSs from waste tire powder at 900 °C for 0.25 h (S1; (a)) and 800 °C for 3 h (S2; (b)) in N_2 atmosphere.

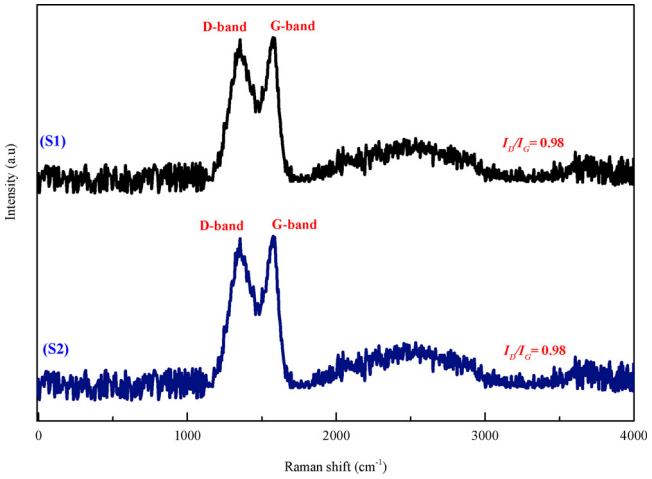

Fig. 5. Raman spectra of the as-synthesized CNSs from waste tire powder at 900 °C for 0.25 h (S1) and 800 °C for 3 h (S2) in N_2 atmosphere.

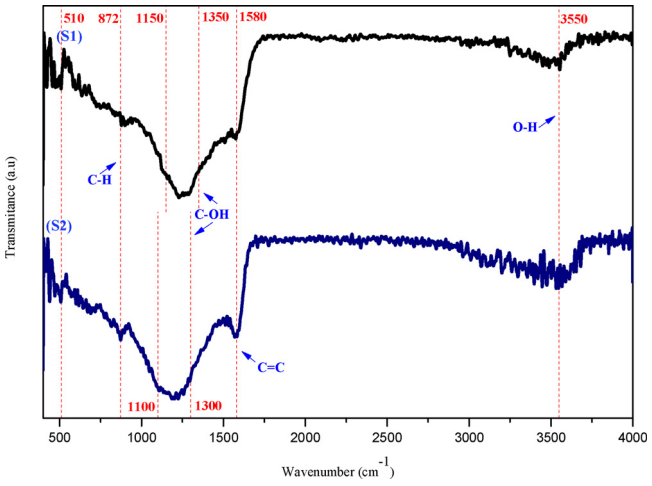

Fig. 6. FTIR spectra of the as-synthesized CNSs from waste tire powder at 900 °C for 0.25 h (S1) and 800 °C for 3 h (S2) in N_2 atmosphere.

which were synthesized from sucrose at 2300 °C through a spray pyrolysis method [76]. Besides, the pore size distribution plots of both samples exhibit multimodal pore size distribution with a size in the range of 1 − 100 nm. The mean pore diameter for S1 and S2 have obtained 44.9 and 25.6 nm, respectively. BET surface area is one of the most important textural properties of the CNSs. The BET surface area for S_1 and S_2 were 65 and 124 m^2/g, respectively. The high specific surface area was acquired wthe ith the longer carbonization time (S_2 sample) due to Boudouard reaction which is a suitable reaction for development of higher internal porosity. Similar specific surface area values (78.6 and 117.7 m^2/g.) were found by Maroufi et al. [22] from the transformation of the waste tire at 1550 °C. Besides, the total pore volume of S1 and S2 samples was found to be 0.73 and 0.79 cm3/g, respectively. These findings are consistent with those of Maroufi et al. [65]. The pore size distribution (Fig S1 b) shows the pore diameter of 38.53 and 1.29 nm for S_1 and S_2 samples, respectively, confirming the mesoporous and microporous nature. The obtained BET surface area in this study was compared with some literature. The type of precursors and reaction conditions (e.g., temperature and residence time) affects the specific surface area. For example, Maroufi et al. [22] synthesized CNSs with the surface area from 78.6 m^2/g to 117.7 m^2/g by various reaction times (5 s to 20 min) at 1550 °C. Gong et al. [20] reported CNSs with 111 − 227 m^2/g from catalytic pyrolysis of polystyrene. Hegde et al. [66] prepared the CNSs with a BET surface area of 58 m^2/g from catalyst-free pyrolysis of Sago bark for the residence time of 2 h.

3.1.6. Growth mechanism of the CNSs

Based on the literature and the above results, a pathway, which follows the adsorption-diffusion- precipitation model, can be proposed for the growth of CNSs [5,77]. Indeed, the metal catalyst used in the CVD process acted as a template for carbon deposition and graphitization. According to this model, once the reaction temperature increased, Fe and C atoms are firstly generated from the pyrolysis of the ferrocene (catalyst) and the carbonized waste tire (carbon source). Small carbon fragments were then accumulated around Fe nanoparticles. The formed carbon layer directly reacted with each other, due to the high activity, to form graphite sheets. Finally, the CNSs is made through the thickening of the carbon coat during the smooth cooling down of the reactor.

3.2. Environmental assessment of the synthesis process

For CNSs production, the steps of feedstock preparation, feedstock carbonization, CNSs synthesis, and CNSs purification were considered. The inventory related to the stages, including raw materials, transport, and electricity were summarized in Table S1. Fig. 7 presents the relative impact contributions of the four relevant steps of CNSs production in the categories analyzed. As the figure shows, the contribution of each production phase to the environmental impact categories is relatively similar. The feedstock production step presented the highest resource use, energy carriers impact (43 % out of 1.47 MJ), this is due to the use of diesel and electricity in the waste tire recycling process. For electricity consumption, the tire powder carbonization resulted in the most significant environmental indicators of climate change (44 % out of 0.085 kg CO_2 eq). Ozone depletion (72 % out of -1.45E-8 kg CFC11 eq) and land use (100 % out of 1.63 Pt) were the most crucial impact categories resulting from CNSs synthesis and CNSs purification phases, respectively. For the S2, the majority of the impact was mainly due to the CNSs synthesis phase. In other word, the CNSs synthesis phase exhibited the maximum environmental impact regarding the majority of indicators investigated in this work, particularly for eutrophication freshwater (84.7 % out of 3.1E-5 kg P eq), climate change (78.2 % out of 0.255 kg CO_2 eq), acidification terrestrial and freshwater (76.8 % out of 0.0013 mol H^+ eq), and resource use, energy carriers (69.5 % out of 5.09 MJ). The electricity consumption in the process was the main contribution (more than 70 %) for the categories mentioned above. Cossutta et al. [56] investigated the LCA of graphene production at a laboratory scale by a CVD method. They concluded that the electricity requirement quantity of the system had a significant effect on the magnitude of impact categories. Healy et al. [78] found also similar results for environmental assessment of single-walled carbon nanotube processes. Among the processes, the waste tire powder carbonization displayed the least indicators values (less than 3 % of all).

Fig S2 presents the details of the positive and/or negative contributions of each subsystem to the environmental impacts of the CNSs. Overall; electricity consumption is a major contributor to the environmental burdens of the CNSs system (highest impact in more than 11 of the 16 categories). Its contribution differs from 2 % (RUMM) to 74 % (EF) for S1 and from 4 % (RUMM) to 87 % (EF) for S2. Besides, according to CED, a total of 3.7 and 5.9 MJ were required to produce 1 g of S1 and S2, respectively, in which 3.3 and 5.3 MJ were non-renewable energy and the remaining parts were renewable. These results are consistent with Cossutta et al. [56]' s research. They reported the LCA of three graphene production routes and concluded that electricity input is the main factor in specifying life cycle environmental burdens. Therefore, focusing on energy consumption decreasing to improve the environmental performance of the system as a whole is suggested. To be more precise, the temperature and the time required for the feedstock conversion process and CNSs synthesis should be declined due to their direct dependence on electric power consumption. An optimistic

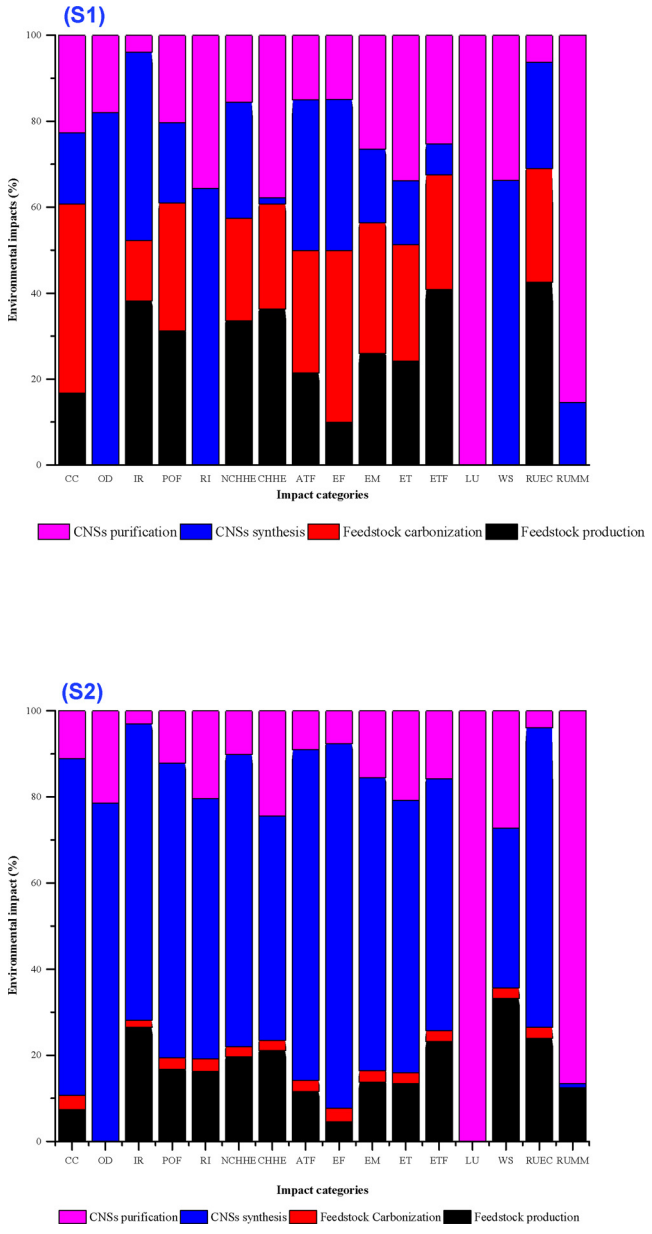

Fig. 7. Contribution of the CNSs synthesis processes from waste tire powder to the environmental impacts.

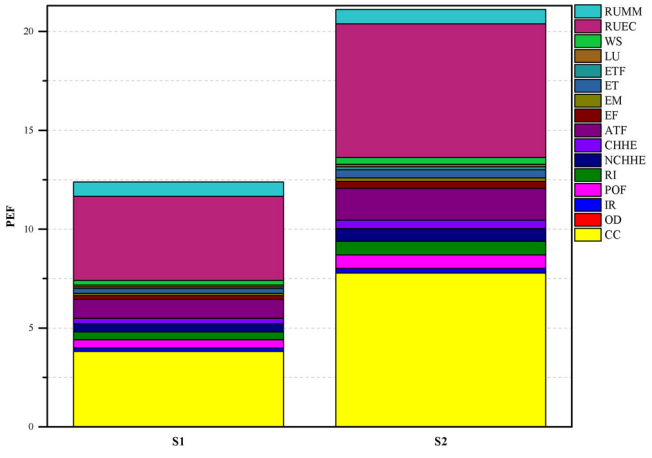

Fig. 8. Comparison of PEF results of CNSs samples synthesized from waste tire powder.

solution is that all electricity be generated from renewable resources. Another relevant contributor to indicators was acid consumption (HCl and HNO_3) in the system. RUMM, NCHHE, CHHE, and CC were the main environmental burden of using acids for CNSs purification. These results, therefore, show the importance of the type and quantity of acid in creating environmental problems, recovery, and reuse of acids where feasible in order to reduce them. In order to compare the environmental proficiency of two samples and identify the most impact or hot spots, the PEF method was investigated. Fig. 8 depicts the normalized results for the 16 impact categories of samples. S2 had a larger PEF value of 21.1 than the S1 quantity of 12.3. The PEF of S2 was 41 % higher than S1. The maximum impact category contributions were exhibited in climate change and resource use, energy carriers, which were at least 30 % to the result in each sample. For graphene synthesis, Cossutta et al. [56] found that the climate change category was the dominant metric, with 2–3 orders of magnitude greater than the other environmental burdens. The lowest impacts happened in ozone depletion (-0.02 for S1 and -0.007 for S2).

Fig. S3 in SI presents the CML 2001 normalized environmental impacts results of as-synthesized CNSs. As shown in this figure, the ionizing radiation (IR) had the greatest environmental impact throughout the life cycle of CNSs (for both samples). It is measured in terms of disability-adjusted life year (DALYs). The damage generated from 1 g of CNSs were calculated about $4.1E^{-10}$ (for S2) and $3.18E^{-10}$ (for S1) DALYs. It might be related to the radionuclides such as carbon-14, cesium-134, cobalt-58, and etc. which are released during energy (e.g., diesel) and hexane production.

The emitted radioactive nuclide can be inhaled by humans and lead to various types of cancer and birth defects [79]. Besides, terrestrial ecotoxicity (TE), freshwater aquatic ecotoxicity (FWAE), and marine aquatic ecotoxicity (MAE) were the major environmental impact groups of both samples. The tire textiles and electricity were the main contributors to TE, FWAE, and MAE indicators, respectively. The acidification (AC) potential with the value of 0.0007 (for S1) and 0.0012 (for S2) kg SO_2 eq per one g of CNSs had also a high rank in the life cycle of CNSs production. This is due to the emission of sulfur dioxide from electricity consumption in the manufacturing system. Moreover, the quantity of the global warming potential for S1 and S2 samples were obtained 0.14 and 0.28 kg CO_2-eq per functional unit, respectively. The calculated measures were near to that obtained by PEF methods. It is ascribed to the greenhouse gas emissions such as CO_2, CH_4, etc. produced during fossil fuel combustion for heat and electricity generation. Khanna et al. [52] reported that global warming potential was one of the most important environmental impacts of carbon nanofibers (CNFs) synthesis process. About 0.65 and 0.47 kg CO_2 eq were emitted to produce 1 g methane-based and ethylene-based CNFs, respectively.

4. Conclusion

This research proposed the use of waste tire powder as a precursor for the synthesis of CNSs. The nano-spherical shaped carbons with uniform sizes ranging from 18 to 50 nm and interlayer d-spacing 3.5 nm were prepared successfully. The BET surface area and total pore volume of the CNSs were 65-124 m^2/g and 0.73-0.79 cm^3/g, respectively. Raman and XRD analyses confirmed nanocrystalline carbon with a high graphitization degree. The environmental burdens of the obtained CNSs were calculated for several impact categories by PEF, CML baseline 2001, and CED methods. The results of the PEF method showed that the steps of CNSs preparation had an essential role in the magnitude of indicator categories. The feedstock production (for S1) and CNSs synthesis (for S2) phases exhibited the maximum environmental impact regarding the majority of indicators. According to the CML baseline 2001, ionizing radiation was the most significant environmental impact of CNSs synthesis from waste tire powder (both samples). The damage produced from 1 g of CNSs was estimated at about 4.1E-10 (for S2) and

3.18E-10 (for S1) DALYs. A total CED of 3.7 and 5.9 MJ was required to produce 1 g of S1 and S2 which 89 % of those were non-renewable energy, respectively. Generally, S2 had the largest environmental footprint value of 21.1. Although S2 had the highest BET surface area than S1, it presented the highest environmental impact for most of the impact categories. It can be concluded that electricity consumption is a major contributor to the environmental burdens of the CNSs system. Therefore, to enhance the environmental efficiency of the system, energy consumption should be reduced.

Declaration of competing interest

No conflict of interest exists.

CRediT authorship contribution statement

Ava Heidari: Conceptualization, Methodology, Software, Validation, Formal analysis, Investigation, Resources, Writing - original draft, Visualization, Project administration, Funding acquisition. **Habibollah Younesi:** Validation, Data curation, Writing - review & editing, Supervision.

Acknowledgments

The authors would like to acknowledge the Ferdowsi University of Mashhad, Iran. (FUM) (Research ID 40085) for its financial support.

Appendix A. Supplementary data

Supplementary material related to this article can be found, in the online version, at doi:https://doi.org/10.1016/j.jece.2020.103669.

References

[1] V. Georgakilas, J.A. Perman, J. Tucek, R. Zboril, Broad family of carbon nanoallotropes: classification, chemistry, and applications of fullerenes, carbon dots, nanotubes, graphene, nanodiamonds, and combined superstructures, Chem. Rev. 115 (2015) 4744–4822.
[2] P. Serp, M. Corrias, P. Kalck, Carbon nanotubes and nanofibers in catalysis, Appl. Catal. A Gen. 253 (2003) 337–358.
[3] M. Inagaki, M. Toyoda, Y. Soneda, S. Tsujimura, T. Morishita, Templated mesoporous carbons: synthesis and applications, Carbon 107 (2016) 448–473.
[4] G. Madhura Mohan, S. Rakesh Ravindra, Fullerenes: chemistry and its applications, Mini. Org. Chem. 12 (2015) 355–366.
[5] A.A. Deshmukh, S.D. Mhlanga, N.J. Coville, Carbon spheres, Mater. Sci. Eng. R Rep. 70 (2010) 1–28.
[6] A.A. Alazemi, V. Etacheri, A.D. Dysart, L.-E. Stacke, V.G. Pol, F. Sadeghi, Ultrasmooth submicrometer carbon spheres as lubricant additives for friction and wear reduction, ACS Appl. Mater. Interfaces 7 (2015) 5514–5521.
[7] L. Dai, D.W. Chang, J.-B. Baek, W. Lu, Carbon nanomaterials for advanced energy conversion and storage, Small 8 (2012) 1130–1166.
[8] J. Han, G. Xu, B. Ding, J. Pan, H. Dou, D.R. MacFarlane, Porous nitrogen-doped hollow carbon spheres derived from polyaniline for high performance supercapacitors, J. Mater. Chem. A 2 (2014) 5352–5357.
[9] G. Zheng, S.W. Lee, Z. Liang, H.W. Lee, K. Yan, H. Yao, H. Wang, W. Li, S. Chu, Y. Cui, Interconnected hollow carbon nanospheres for stable lithium metal anodes, Nat. Nanotechnol. 9 (2014) 618–623.
[10] S. Kapri, R. Majee, S. Bhattacharyya, Chemical modifications of porous carbon nanospheres obtained from ubiquitous precursors for targeted drug delivery and live cell imaging, ACS Sustain. Chem. Eng. 6 (2018) 8503–8514.
[11] J.-Y. Miao, D.W. Hwang, K.V. Narasimhulu, P.-I. Lin, Y.-T. Chen, S.-H. Lin, L.-P. Hwang, Synthesis and properties of carbon nanospheres grown by CVD using Kaolin supported transition metal catalysts, Carbon 42 (2004) 813–822.
[12] S. Supriya, A. Divyashree, S. Yallappa, G. Hegde, Carbon nanospheres obtained from carbonization of bio-resource: a catalyst free synthesis, Materials Today: Proceedings (2018) 2907–2911 5.
[13] W.M. Qiao, Y. Song, S.Y. Lim, S.H. Hong, S.H. Yoon, I. Mochida, T. Imaoka, Carbon nanospheres produced in an arc-discharge process, Carbon 44 (2006) 187–190.
[14] K. Niwase, T. Homae, K.G. Nakamura, K. Kondo, Generation of giant carbon hollow spheres from C60 fullerene by shock-compression, Chem. Phys. Lett. 362 (2002) 47–50.
[15] Y. Ma, Z. Hu, K. Huo, Y. Lu, Y. Hu, Y. Liu, J. Hu, Y. Chen, A practical route to the production of carbon nanocages, Carbon 43 (2005) 1667–1672.
[16] N. Koprinarov, M. Konstantinova, Preparation of carbon spheres by low-temperature pyrolysis of cyclic hydrocarbons, J. Mater. Sci. 46 (2011) 1494–1501.
[17] S.A.A. Manaf, P. Roy, K.V. Sharma, Z. Ngaini, V. Malgras, A. Aldalbahi, S.M. Alshehri, Y. Yamauchi, G. Hegde, Catalyst-free synthesis of carbon nanospheres for potential biomedical applications: waste to wealth approach, RSC Adv. 5 (2015) 24528–24533.
[18] S. Chandra Kishore, S. Anandhakumar, M. Sasidharan, Direct synthesis of solid and hollow carbon nanospheres over NaCl crystals using acetylene by chemical vapour deposition, Appl. Surf. Sci. 400 (2017) 90–96.
[19] Z. Zhong, H. Chen, S. Tang, J. Ding, J. Lin, K. Lee Tan, Catalytic growth of carbon nanoballs with and without cobalt encapsulation, Chem. Phys. Lett. 330 (2000) 41–47.
[20] J. Gong, J. Liu, X. Chen, X. Wen, Z. Jiang, E. Mijowska, Y. Wang, T. Tang, Synthesis, characterization and growth mechanism of mesoporous hollow carbon nanospheres by catalytic carbonization of polystyrene, Microporous Mesoporous Mater. 176 (2013) 31–40.
[21] R. Atchudan, S. Perumal, T.N. Jebakumar Immanuel Edison, Y.R. Lee, Facile synthesis of monodisperse hollow carbon nanospheres using sucrose by carbonization route, Mater. Lett. 166 (2016) 145–149.
[22] S. Maroufi, M. Mayyas, V. Sahajwalla, Nano-carbons from waste tyre rubber: an insight into structure and morphology, Waste Manag. 69 (November) (2017) 110–116.
[23] Y.-R. Lin, H. Teng, Mesoporous carbons from waste tire char and their application in wastewater discoloration, Microporous Mesoporous Mater. 54 (2002) 167–174.
[24] Y. Zhang, C. Wu, M.A. Nahil, P. Williams, High-value resource recovery products from waste tyres, Proceedings of the Institution of Civil Engineers - Waste and Resource Management 169 (2016) 137–145.
[25] H. Teng, M.A. Serio, M.A. Wojtowicz, R. Bassilakis, P.R. Solomon, Reprocessing of used tires into activated carbon and other products, Ind. Eng. Chem. Res. 34 (1995) 3102–3111.
[26] B. Acevedo, C. Barriocanal, Texture and surface chemistry of activated carbons obtained from tyre wastes, Fuel Process. Technol. 134 (2015) 275–283.
[27] M. Betancur, J.D. Martínez, R. Murillo, Production of activated carbon by waste tire thermochemical degradation with CO2, J. Hazard. Mater. 168 (2009) 882–887.
[28] J.-H. Lin, S.-B. Wang, An effective route to transform scrap tire carbons into highly-pure activated carbons with a high adsorption capacity of ethylene blue through thermal and chemical treatments, Environ. Technol. Innov. 8 (2017) 17–27.
[29] T.A. Saleh, V.K. Gupta, Processing methods, characteristics and adsorption behavior of tire derived carbons: a review, Adv. Colloid Interface Sci. 211 (2014) 93–101.
[30] P.T. Williams, Pyrolysis of waste tyres: a review, Waste Manag. 33 (2013) 1714–1728.
[31] M. Sienkiewicz, J. Kucinska-Lipka, H. Janik, A. Balas, Progress in used tyres management in the European Union: a review, Waste Manag. 32 (2012) 1742–1751.
[32] Z. Derakhshan, M.T. Ghaneian, A.H. Mahvi, G. Oliveri Conti, M. Faramarzian, M. Dehghani, M. Ferrante, A new recycling technique for the waste tires reuse, Environ. Res. 158 (2017) 462–469.
[33] D. Czajczyńska, R. Krzyżyńska, H. Jouhara, N. Spencer, Use of pyrolytic gas from waste tire as a fuel: A review, Energy.
[34] M. Sabzekar, G. Zohuri, M.P. Chenar, S.M. Mortazavi, M. Kariminejad, S. Asadi, A new approach for reclaiming of waste automotive EPDM rubber using waste oil, Polym. Degrad. Stab. 129 (2016) 56–62.
[35] S. Li, C. Wan, X. Wu, S. Wang, Core-shell structured carbon nanoparticles derived from light pyrolysis of waste tires, Polym. Degrad. Stab. 129 (2016) 192–198.
[36] W. Qu, Q. Zhou, Y.-Z. Wang, J. Zhang, W.-W. Lan, Y.-H. Wu, J.-W. Yang, D.-Z. Wang, Pyrolysis of waste tire on ZSM-5 zeolite with enhanced catalytic activities, Polym. Degrad. Stab. 91 (2006) 2389–2395.
[37] W. Yang, W.J. Sun, W. Chu, C.F. Jiang, J. Wen, Synthesis of carbon nanotubes using scrap tyre rubber as carbon source, Chin. Chem. Lett. 23 (2012) 363–366.
[38] Y. Zhang, P.T. Williams, Carbon nanotubes and hydrogen production from the pyrolysis catalysis or catalytic-steam reforming of waste tyres, J. Anal. Appl. Pyrolysis 122 (2016) 490–501.
[39] R.W. Kates, W.C. Clark, R. Corell, J.M. Hall, C.C. Jaeger, I. Lowe, J.J. McCarthy, H.J. Schellnhuber, B. Bolin, N.M. Dickson, S. Faucheux, G.C. Gallopin, A. Grubler, B. Huntley, J. Jager, N.S. Jodha, R.E. Kasperson, A. Mabogunje, P. Matson, H. Mooney, B. Moore 3rd, T. O'Riordan, U. Svedlin, Environment and development, Sustain. Sci. Sci. (New York, N.Y.) 292 (2001) 641–642.
[40] M.S. Diallo, N.A. Fromer, M.S. Jhon, Nanotechnology for sustainable development: retrospective and outlook, J. Nanoparticle Res. 15 (2013) 2044.
[41] K. Savolainen, H. Alenius, H. Norppa, L. Pylkkänen, T. Tuomi, G. Kasper, Risk assessment of engineered nanomaterials and nanotechnologies—a review, Toxicology 269 (2010) 92–104.
[42] H. Şengül, T.L. Theis, S. Ghosh, Toward sustainable nanoproducts, J. Ind. Ecol. 12 (2008) 329–359.
[43] D.E. Meyer, M.A. Curran, M.A. Gonzalez, An examination of existing data for the industrial manufacture and use of nanocomponents and their role in the life cycle impact of nanoproducts, Environ. Sci. Technol. 43 (2009) 1256–1263.
[44] M.R. Wiesner, G.V. Lowry, P. Alvarez, D. Dionysiou, P. Biswas, Assessing the risks of manufactured nanomaterials, Environ. Sci. Technol. 40 (2006) 4336–4345.
[45] V. Türk, C. Kaiser, S. Schaller, Invisible but tangible? Societal opportunities and risks of nanotechnologies, J. Clean. Prod. 16 (2008) 1006–1009.
[46] J.M. Balbus, K. Florini, R.A. Denison, S.A. Walsh, Protecting workers and the environment: an environmental NGO's perspective on nanotechnology, J. Nanoparticle Res. 9 (2007) 11–22.
[47] R. Hischier, T. Walser, Life cycle assessment of engineered nanomaterials: state of the art and strategies to overcome existing gaps, Sci. Total Environ. 425 (2012) 271–282.
[48] E.I. ISO, Environmental Management - Life Cycle Assessment - Principles and framework., ISO 14040, European Standard, (2006).

[49] W. Marimón-Bolívar, E.E. González, Green synthesis with enhanced magnetization and life cycle assessment of Fe3O4 nanoparticles, Environ. Nanotechnol. Monit. Manag. 9 (2018) 58–66.
[50] F.A. Deorsola, N. Russo, G.A. Blengini, D. Fino, Synthesis, characterization and environmental assessment of nanosized MoS2 particles for lubricants applications, Chem. Eng. J. 195–196 (2012) 1–6.
[51] V. Khanna, B.R. Bakshi, Carbon nanofiber polymer composites: evaluation of life cycle energy use, Environ. Sci. Technol. 43 (2009) 2078–2084.
[52] V. Khanna, B.R. Bakshi, L.J. Lee, Carbon nanofiber production, J. Ind. Ecol. 12 (2008) 394–410.
[53] S. Gavankar, S. Suh, A.A. Keller, The role of scale and technology maturity in life cycle assessment of emerging technologies: a case study on carbon nanotubes, J. Ind. Ecol. 19 (2015) 51–60.
[54] M.J. Eckelman, M.S. Mauter, J.A. Isaacs, M. Elimelech, New perspectives on nanomaterial aquatic ecotoxicity: production impacts exceed direct exposure impacts for carbon nanotoubes, Environ. Sci. Technol. 46 (2012) 2902–2910.
[55] G. Rodriguez-Garcia, B. Zimmermann, M. Weil, Nanotoxicity and life cycle assessment: first attempt towards the determination of characterization factors for carbon nanotubes, IOP Conference Series: Materials Science and Engineering 64 (2014) 012029.
[56] M. Cossutta, J. McKechnie, S.J. Pickering, A comparative LCA of different graphene production routes, Green Chem. 19 (2017) 5874–5884.
[57] A.D. Ampah, E. Pagone, K. Salonitis, Life Cycle Assessment of Graphene as Heating Element, Springer Singapore, Singapore, 2019, pp. 283–297.
[58] M. Miseljic, S.I. Olsen, Life-cycle assessment of engineered nanomaterials: a literature review of assessment status, J. Nanoparticle Res. 16 (2014) 2427.
[59] Y. Pu, F. Tang, P.-M. Adam, B. Laratte, R.E. Ionescu, Fate and characterization factors of nanoparticles in seventeen subcontinental freshwaters: a case study on copper nanoparticles, Environ. Sci. Technol. 50 (2016) 9370–9379.
[60] M. Pini, B. Salieri, A.M. Ferrari, B. Nowack, R. Hischier, Human health characterization factors of nano-TiO2 for indoor and outdoor environments, Int. J. Life Cycle Assess. 21 (2016) 1452–1462.
[61] Y. Deng, J. Li, M. Qiu, F. Yang, J. Zhang, C. Yuan, Deriving characterization factors on freshwater ecotoxicity of graphene oxide nanomaterial for life cycle impact assessment, Int. J. Life Cycle Assess. 22 (2017) 222–236.
[62] A.L. Patterson, The scherrer formula for X-Ray particle size determination, Phys. Rev. 56 (1939) 978–982.
[63] T. Gao, B.P. Jelle, L.I.C. Sandberg, A. Gustavsen, Monodisperse hollow silica nanospheres for nano insulation materials: synthesis, characterization, and life cycle assessment, ACS Appl. Mater. Interfaces 5 (2013) 761–767.
[64] EC, The European Commission, 2013/179/EU: commission r ecommendation of 9 April 2013 on the use of common methods to measure and communicate the life cycle environmental performance of products and organizations, Orkesterjournalen 124 (2013) 1–210.
[65] S. Maroufi, M. Mayyas, V. Sahajwalla, Nano-carbons from waste tyre rubber: an insight into structure and morphology, Waste Manag. 69 (2017) 110–116.
[66] G. Hegde, S.A. Abdul Manaf, A. Kumar, G.A.M. Ali, K.F. Chong, Z. Ngaini, K.V. Sharma, Biowaste sago bark based catalyst free carbon nanospheres: waste to wealth approach, ACS Sustain. Chem. Eng. 3 (2015) 2247–2253.
[67] J. Kang, O.L. Li, N. Saito, Synthesis of structure-controlled carbon nano spheres by solution plasma process, Carbon 60 (2013) 292–298.
[68] Y. Li, J. Chen, Q. Xu, L. He, Z. Chen, Controllable route to solid and hollow monodisperse carbon nanospheres, J. Phys. Chem. C 113 (2009) 10085–10089.
[69] Y. Li, E.J. Lee, W. Cai, K.Y. Kim, S.O. Cho, Unconventional method for morphology-controlled carbonaceous nanoarrays based on Electron irradiation of a polystyrene colloidal monolayer, ACS Nano 2 (2008) 1108–1112.
[70] S. Feshki, M. Marandi, Synthesis of carbon spheres of controlled size by hydrothermal method, J. Nanostructures 4 (2014) 295–301.
[71] L. Zhang, M. Yao, W. Yan, X. Liu, B. Jiang, Z. Qian, Y. Gao, X.J. Lu, X. Chen, Q. Wang, Delivery of a chemotherapeutic drug using novel hollow carbon spheres for esophageal cancer treatment, Int. J. Nanomedicine 12 (2017) 6759–6769.
[72] R. Cui, C. Liu, J. Shen, D. Gao, J.-J. Zhu, H.-Y. Chen, Gold nanoparticle–colloidal carbon nanosphere hybrid material: preparation, characterization, and application for an amplified electrochemical immunoassay, Adv. Funct. Mater. 18 (2008) 2197–2204.
[73] Y. Zhang, M. Dong, S. Zhu, C. Liu, Z. Wen, MnO2@colloid carbon spheres nanocomposites with tunable interior architecture for supercapacitors, Mater. Res. Bull. 49 (2014) 448–453.
[74] M. Thommes, K. Kaneko, V. Neimark Alexander, P. Olivier James, F. Rodriguez-Reinoso, J. Rouquerol, S.W. Sing Kenneth, Physisorption of gases, with special reference to the evaluation of surface area and pore size distribution (IUPAC technical report), Pure Appl. Chem. (2015) 1051.
[75] S.-S. Chang, B. Clair, J. Ruelle, J. Beauchêne, F. Di Renzo, F. Quignard, G.-J. Zhao, H. Yamamoto, J. Gril, Mesoporosity as a new parameter for understanding tension stress generation in trees, J. Exp. Bot. 60 (2009) 3023–3030.
[76] V. Etacheri, C. Wang, M.J. O'Connell, C.K. Chan, V.G. Pol, Porous carbon sphere anodes for enhanced lithium-ion storage, J. Mater. Chem. A 3 (2015) 9861–9868.
[77] B.-S. XU, Prospects and research progress in nano onion-like fullerenes, New Carbon Mater. 23 (2008) 289–301.
[78] M.L. Healy, L.J. Dahlben, J.A. Isaacs, Environmental assessment of single-walled carbon nanotube processes, J. Ind. Ecol. 12 (2008) 376–393.
[79] N.R. Council, Drinking Water and Health vol. 1, The National Academies Press, Washington, DC, 1977.